ORIGINAL ARTICLE

Eur. J. Anat. 19 (1): 15-26 (2015)

Morphology of female guinea pig Harderian gland during postnatal development - secretory endpieces

Sanaa A.M. Elgayar, Amal T. Abou-Elghait and Abderahman A. Sayed

Department of Histology, Faculty of Medicine, Assiut University, Assiut, Egypt

SUMMARY

The main objective of this study was to investigate the morphological aspects of the development of the Harderian gland (HG) in the female guinea pig. A total number of thirty animals were used and divided according to age into groups, five animals each. Specimens were taken at the following ages; birth, one week, two weeks, three weeks, four weeks and two months postnatal. Histological, histochemical and immunohistochemical techniques were used. The gland was constituted of secretory end pieces and a duct system formed of intra- and extra-parenchymal ducts. At birth, the female guinea pig HG was active in the secretion of lipid and neutral mucin and the differentiation of several populations of cells (light and dark) was possible. However, its histological structure was still incomplete. The lining cells revealed many free ribosomes, a few and small organelles and large irregularly shaped nuclei and numerous mitotic figures. The secretory cells reached maturity by the age of three weeks, but growth in size continued up to the age of two months. They were light or dark; the light cells presented three forms that exhibited different morphological features. All modes of secretion (apocrine, merocrine and holocrine) were detected.

Key words: Female guinea pig – Harderian gland – Development

INTRODUCTION

The Harderian gland (HG) is an exocrine gland located behind the ocular bulb in many mammals (Satoh et al., 1996). In rodents this gland is large and contains a considerable amount of lipid and porphyrins secreted via a duct that opens directly into the nictitating membrane (Watanabe, 1980). It has been reported that the gland functions may vary with species (Payne, 1994 in tetrapods; Dejeridane et al., 1996 in mammals; Sakai, 1992 in rodents). The known functions of this gland include: lubrication of the eye, secretion of pheromones, secretion of growth factors, osmoregulation, photoprotection and thermoregulation (Chieffi et al., 1993). Although the HGs of different rodent species share many common features, none are identical. It is stated that the description for each species is different, and the morphology of the gland in any unstudied species could not be inferred safely from existing reports (Payne 1994). Guinea pigs Hg are of particular interest; although they have no nictitating membrane (Smelser, 1943), they possess well-developed HG which does not secrete porphyrin (Seyama et al., 1984). Besides, the guinea pig is more physiologically and immunologically similar to humans than other small animal models (Padilla-Carlin et al., 2008). However, very little is reported on the morphology of guinea pig HG. The only known description of adult guinea pig HG was by Paule (1957), all subsequent guinea pig HG papers being about lipid synthesis (Satoh et al, 1993). Few reports could be found on the development of the HG in rodents (Muller, 1969; Lopez et al., 1990, 1992a,b; Lopez et al., 1996; Wetterberg et al., 1970; Menendez-Pelaez et al., 1992). To the best of the author's knowledge, no reports are available on the development of HG in guinea pig. Therefore, the lack of an in-depth study prompted us to carry out this work which aimed at providing a detailed morphological study of secretory cells in developing fe-

Corresponding author: Sanaa A.M. Elgayar. Department of Histology, Faculty of Medicine, Assiut University, Assiut, 71515, Egypt. Tel: +02(01273636763). E-mail: selgar1@hotmail.com

Submitted: 29 March, 2014. *Accepted:* 12 June, 2014.

male guinea pig HG using light, electron microscopy and immunohistochemistry. The characteristic morphological features of the other structures constituting the parenchyma will be covered in a separate report. As sexual differences of the lipids and their metabolism in the HG of the golden hamster have been reported (Seyama et al., 1995; 1996), only females were studied in this work to avoid the potential gender-related differences in the HG of guinea pig. Understanding the glandular structure in the guinea pig would be helpful in order to study eye physiological processes or diseases.

MATERIALS AND METHODS

A total number of thirty female guinea pigs were used and divided into groups (five animals each): at birth (newborn), one week, two weeks, three weeks, one month (young growing), two months (adolescent) (Chitano et al., 2000). The animals were anesthetized with ether and perfused intracardially with the appropriate fixative (5%) glutaraldehyde for electron microscopy and 10% formalin for light microscopy (LM). After removal of the eye, the HG was dissected out and cut into small pieces.

LM The specimens were immersed into 10% formalin for two days fixation. Next, the specimens were processes for preparation of paraffin blocks. Paraffin sections (5-7 µm) were cut into a transverse plane, mounted into glass slides, and every tenth section was stained with hematoxylin & eosin stain (Drury and Wallington, 1980). In addition, selected sections were processed for histochemical demonstration of polysaccharides using Alcian blue (AB) at PH 2.5 for acid mucosubstances, periodic acid Schiff (PAS) method for neutral mucosubstances, and green staining of mucin by Masson's trichrome stain. Processing and staining techniques were done according to Drury and Wallington (1980).

TEM The specimens were immersed in glutaraldehyde in cacodylate buffer for 24 hours and post fixed in 1% osmium tetroxide in phosphate buffer for two hours. Tissues were rinsed in the same buffer dehydrated with alcohol, cleared with propylene oxide and embedded in epon 812. Semi-thin sections (0.5-1 µm) were cut and stained with toluidine blue (Gupta, 1983) for examination on a light microscope. Ultrathin sections (500-800 Å) were cut from selected areas of the blocks and contrasted with uranyl acetate and lead citrate (Reynolds, 1963). These sections were observed with the transmission electron microscope (Jeol E.M.-100 CX11; Japanese electron optic laboratory, Tokyo, Japan) and photographed at 80 K.V.

Immunohistochemistry Expression of chromogranin A (CgA) was detected in formalin-

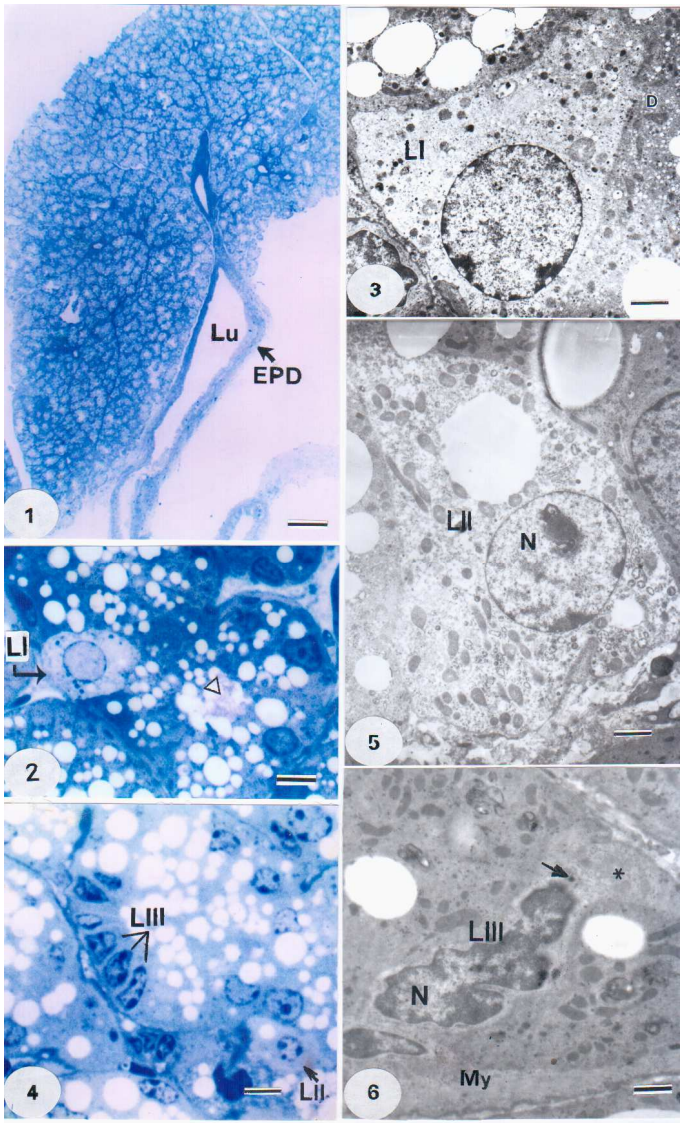

Fig. 1. Semithin section of the newborn Harderian gland (HG) . EPD (extraparenchymal duct), Lu (lumen). Toluidine blue, x 10. Bar, 0.1 µm.

Fig. 2. Semi-thin section in newborn HG, type I light cell (LI), fixed secretion (∆). Toluidine blue, x 1000. Bar, 10 µm.

Fig. 3. TEM from newborn HG showing type I light cell (LI). D (dark cell), L (lipid vacuole). x 5,200. Bar, 1.8 µm.

Fig. 4. Semithin section of newborn HG showing type II light cell (L II), type III light cell (L III). Toluidine blue, x 1000. Bar, 10 µm.

Fig. 5. TEM from newborn HG showing type II light cell (LII) with rounded nucleus (N). x 3,500. Bar, 2.8 µm.

Fig. 6. TEM from newborn HG showing type III light cell (LIII). Basal ovoid irregular nucleus (N), apical cytoplasm (*), a secretory granule (↑), My (myoepithelial cell). x 3,500. Bar, 2.8 µm.

fixed paraffin-embedded sections. Sections (5 µm) were deparaffinized and rehydrated. Sections were digested with protease XXV (enzyme-induced epitope retrieval) at 1 mg/ml PBS solution for 10 minutes at 37˚C. Sections were processed according to the manufacture instructions using the universal kit (ultravision detection system, anti-polyvalent, HRP/DAB, Thermo Fischer Scientific, Fremont, CA, USA). Immunohistochemical staining was demonstrated using labeled streptavidin-biotin immunoperoxide technique. Mouse monoclonal antibody Ab-1 Clone LK2H10 Lab Vision Corp, Neo Markers Inc/ Lab Vision, Fremont, CA, USA) was used at 1:800 dilution for 20 minutes at room temperature. Sections were then incubated with biotinylated goat antipolyvalent secondary antibody for 10 minutes at room temperature. The reaction was then visualized using diaminobenzidine (DAB) for 10 minutes. Sections were counter-stained using Mayer's hematoxylin, dehydrated and cover slipped using a mixture of distyrene (a polystyrene), a plasticizer (tricresyl phosphate), and xylene (DPX).

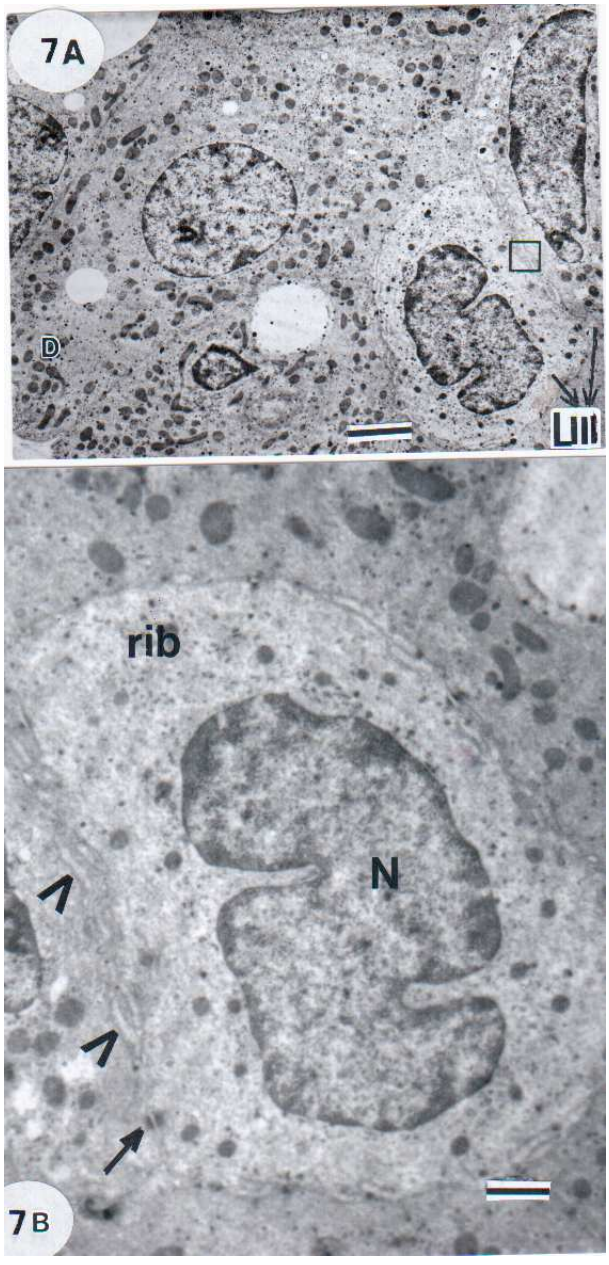

RESULTS

Birth to week one

In newborn animals, the HG was surrounded by a thin capsule. It had a convex surface and a concave hilum from which an extra-parenchymal duct exits (Fig. 1). The secretory end pieces consisted of alveoli or tubuloalveoli lined by a single layer of cuboidal to columnar epithelial cells surrounded by myoepithelial cells. The lining cells contained cytoplasmic vacuoles of variable sizes. Numerous mitotic figures were encountered (Fig. 10) however, their incidence decreased gradually to become rare by the age of three week. According to staining affinity, two types of lining secretory epithelial cells could be distinguished; dark and light. Three forms of light cells were identified and designated; I, II & III (Figs. 2, 4).

Type I light cells were frequently encountered. They possessed large, round, pale basal nuclei surrounded by poorly stained voluminous cytoplasm containing a few dark granules and lipid vacuoles (Fig. 2). In ultrastructure, they contained euchromatic, round central nuclei which were large relative to the cytoplasm, and a few organelles (Fig. 3).

Type II light cells were columnar or pyramidal in shape. They possessed round basal nuclei surrounded by light abundant cytoplasm and some lipid vacuoles (Fig. 4). In ultrastructure, the nuclei were euchromatic with prominent nucleoli and surrounded by copious cytoplasm which contained numerous tiny vesicles and variable sized mitochondria, which may exhibit electron lucent matrix, a scanty short segments of rough endoplasmic reticulum (RER) and lipid vacuoles (Fig. 5).

Type III light cells were high cuboidal or columnar in shape containing dark ovoid nuclei with an irregular outline. The nucleus was large relative to the cytoplasm which was devoid of lipid vacuoles (Fig 4). They were present either singly or in groups. In ultrastructure, the nuclei were heterochromatic and surrounded by a scanty electron lucent cytoplasm containing numerous free ribosomes, mitochondria and a few small electron dense secretory granules. The surrounding plasma membrane exhibited interdigitations and desmosomal junctions with adjacent cells (Figs. 6, 7).

Fig. 7. (A) TEM from one-week Harderian gland (HG) showing type III light cells (LIII) with interdigitations (□). x 2,700. Bar, 3.7 µm. **(B)** TEM from one-week HG showing type III light cells at higher magnification. Oval irregular nucleus (N), free ribosomes (rib), interdigitations (►) and desmosome (↑) between light cells. x 7,200. Bar, 1.4 µm.

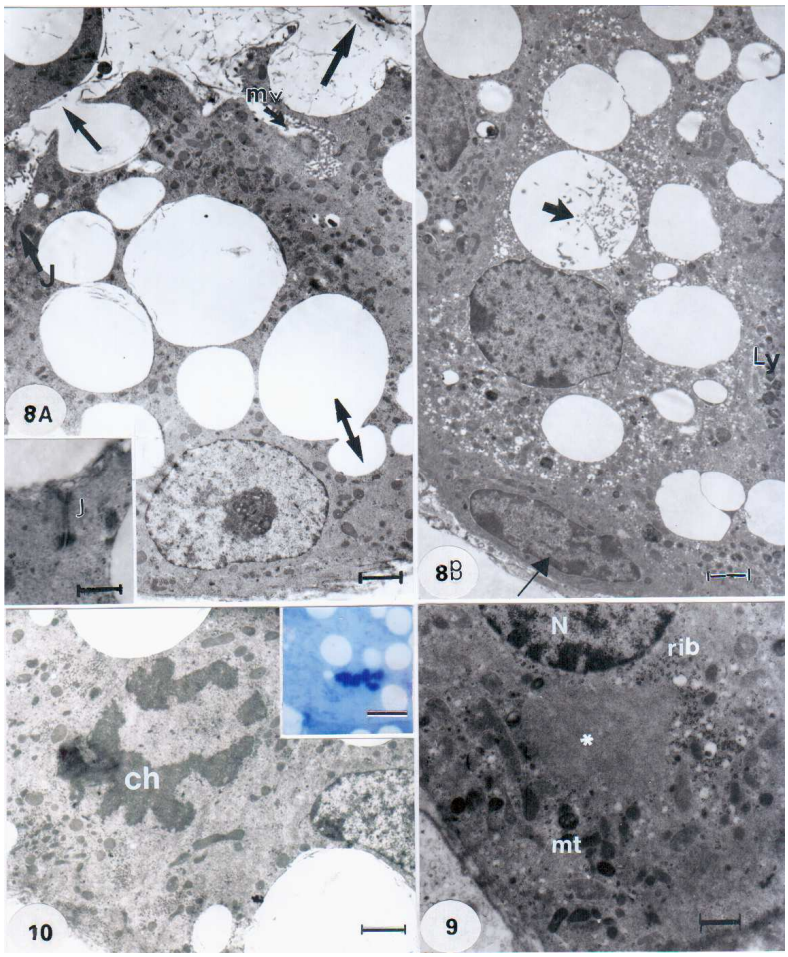

Fig. 8. (A) TEM from newborn Harderian gland (HG) showing a dark cell containing lipid vacuoles opening into the lumen (↑), coalescence of lipid vacuoles (↕), microvilli (mv) and apical junctional complex (J). x 3,500. Bar, 2.8 µm. Inset: High magnification for an apical junctional complex between adjacent dark cells (J). x 14,000. Bar, 0.7 µm. **(B)** TEM from newborn HG showing a dark cell containing numerous smooth vesicles with or without electron dense core, lipid vacuoles with electron dense granular secretion (bold arrow). Lysosomes (Ly), myoepithelial cell (↑). x 3,500. Bar, 2.8 µm.

Fig. 9. TEM from newborn HG showing a part of a dark cell containing nucleolus-like body (*) surrounded by free ribosomes (rib). Nucleus (N), mitochondria (mit). x 8,000. Bar, 1.2 µm.

Fig. 10. TEM from newborn HG. A secretory cell in mitosis, ch (chromosome). x 4,000. Bar, 2.5 µm. Inset: Semi-thin section in new borne HG showing a mitotic figure. Toluidine blue, x 1000. Bar, 10 µm.

Dark cells, which were the most common type, possessed variable-shaped basal nuclei and numerous cytoplasmic lipid vacuoles of variable size. In ultrastructure the apical plasma membrane exhibited unevenly distributed short microvilli (Fig. 8A) and the apical part of the lateral plasma membrane formed junctional complex with the adjacent cells. The cytoplasm contained numerous variable-sized lipid vacuoles that opened into the lumen which may contain some electron-dense granulated secretory material. Other organelles included small mitochondria, free ribosomes and a few short segments of RER, and vesicular smooth endoplasmic reticulum (SER) and lysosomes (Fig. 8A). Some dark cells contained numerous cytoplasmic clear vesicles and electron-dense secretory granules surrounded by a thin membrane (Fig. 8B). Occasionally, the dark cells may reveal nucleolus-like cytoplasmic inclusions which consisted of aggregate of medium density granules without limiting membrane, but a considerable amount of clustered ribosomes were evident (Fig. 9).

The secretory material in the lumina of the secretory end pieces and/or the cytoplasm of the lining cells may reveal PAS positive reaction (Fig. 11) and green colour in Masson's trichrome stain, but AB stain was negative. Apical protrusions extended from the apical surfaces into the lumina (Fig. 13, inset). These protrusions may exhibit metachromatic stained areas in toluidine blue stained semi-thin sections (Fig. 13, inset) and granular electron-dense secretory material in ultrastructure (Fig. 13). Less frequently the lumina of the secretory end pieces and/ or those of the intraparenchymal ducts may exhibit cell nuclei (Figs. 14A, B). In ultrastructure, type II light cells may reveal rupture with release of secretion, which may include granular electron-dense secretory material, into the lumina suggesting holocrine secretion. These cells usually exhibit small heterochromatic nuclei (Fig. 15). The cytoplasmic vacuoles may contain granular electron dense secretory material (Fig. 15).

Myoepithelial cells, which were located at the basal part of secretory end pieces varied in shape, often elongated, with their longitudinal axis oriented parallel to the basement membrane and contained ovoid or elongated nuclei. Their staining affinity varied, being either light (Fig. 16) or dark (Fig. 17) with preponderance of the light one. Mitotic activity was evident in myoepithelial cells which divided symmetrically across their long axis (Fig. 16). In ultrastructure, they were present between the luminal cells and the basal lamina. Their cytoplasm varied in electron density: the majority had low electron density, large nucleus relative to the cytoplasm and a few organelles. These included free ribosomes, filaments, mitochondria (Fig. 16) and centrioles. The dark myoepithelial cells had moderate electron-dense cytoplasm, smaller nucleus and more cytoplasm containing more organelles (Fig. 17).

Lymphocytes were frequently encountered within the secretory end pieces in a basal loca-

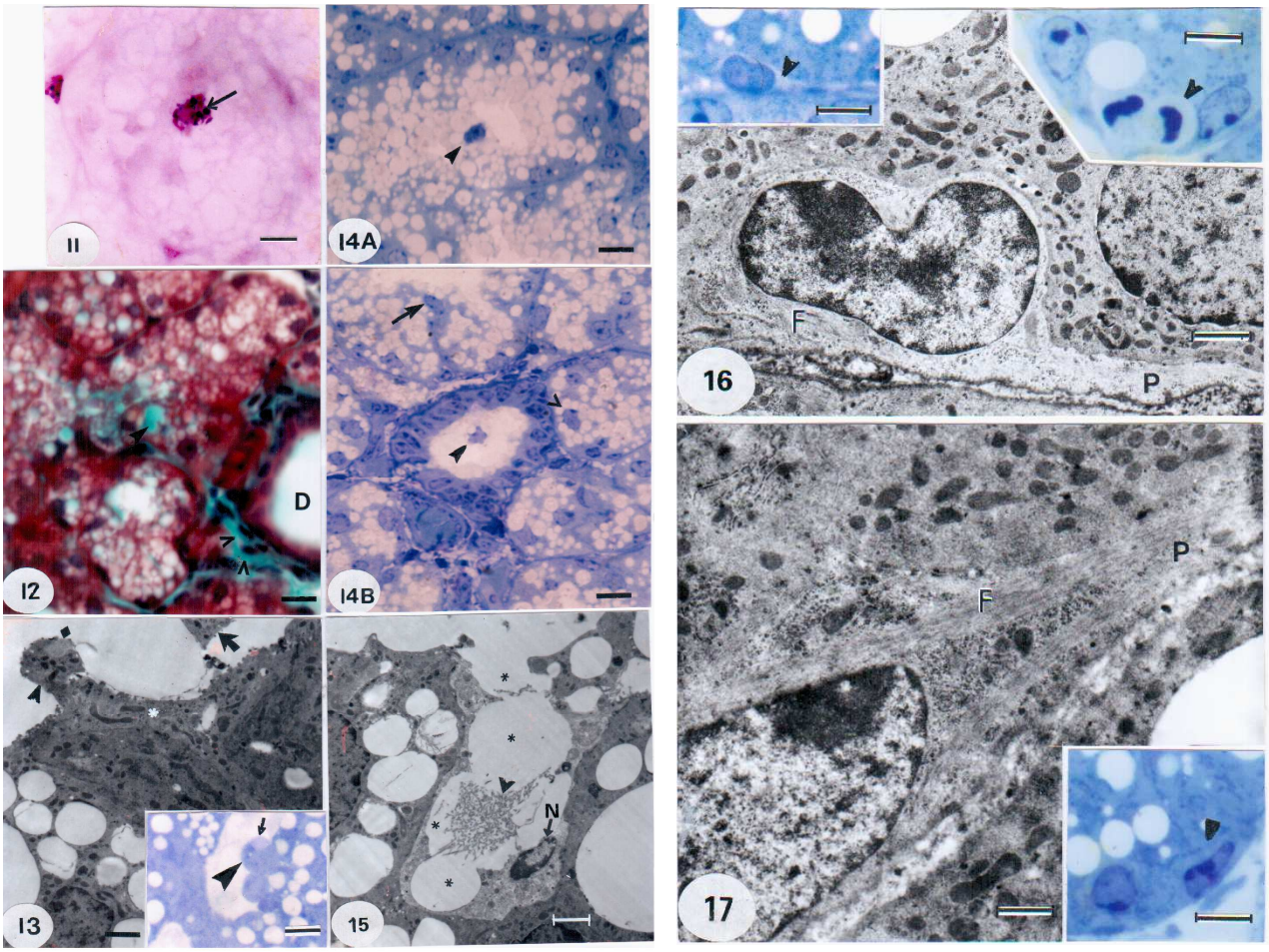

Fig. 11. Paraffin section in newborn Harderian gland (HG) showing PAS positive secretion in a secretory end piece (arrow). PAS, x 1000. Bar, 10 µm.

Fig. 12. Paraffin section in newborn HG showing green stained secretion in secretory end pieces (arrowheads) and collagen fibers (V) around an interlobular duct (D). Masson`s trichrome stain, x 400. Bar, 25 µm.

Fig. 13. TEM from newborn HG showing an apical protrusion (arrowhead) with a thin stalk extending from a dark cell containing granular electron dense secretion (♦) and another released apical protrusion (arrow). x 4,800. Bar, 2 µm. Inset: Semi-thin section in newborn HG showing an apical protruding secretion (arrowhead) with a metachromatic stained part (arrow). Toluidine blue, x 1000. Bar, 10 µm.

Fig. 14. (A) Semithin section in newborn HG showing an epithelial cell studded with cytoplasmic vacuoles and the nucleus is located at the cell surface. Toluidine blue, x 400. Bar = 25 µm. **(B)** Semi-thin section in newborn HG showing an intralobular duct containing luminal remnants of cells with nuclei (arrowhead). The secretory end pieces exhibit cells with an apically displaced nucleus (arrow) and cells full of cytoplasmic vacuoles (empty arrowhead). Toluidine blue, x 400. Bar, 25 µm.

Fig. 15. TEM from newborn HG showing a ruptured type II light cell with a nucleus (N), lipid vacuoles (*) and granular electron dense secretion (arrowhead). x 4,800. Bar, 2 µm.

Fig. 16. TEM from newborn HG showing a Light myoepithelial cell, cytoplasmic process (P), filaments (F). x 6,500. Bar, 1.4 µm. Left inset: semi-thin section in new born HG showing a light myoepithelial cell (arrowhead). Toluidine blue, x 1000. Bar, 10 µm. Right inset: Semi-thin section in new born HG showing a myoepithelial cell in mitosis (arrowhead). Toluidine blue, x 1000. Bar, 10 µm.

Fig. 17. TEM from newborn HG showing a dark myoepithelial cell, cytoplasmic process (P) and a bundle of filaments (F). x 8,700. Bar, 1.1 µm. Inset: semi-thin section in new born HG showing a dark myoepithelial cell (arrowhead). Toluidin blue, x 1000. Bar, 10 µm.

tion between myoepithelial cells and secretory epithelial cells.

Weeks two to three

Type I light cells possessed the same morphological features found in the previous age group; large pale nuclei surrounded by light cytoplasm; however, they became less frequently detectable. In ultrastructure they contained euchromatic nuclei and a few organelles. Type II light cells revealed further growth with a marked increase in amount of granular cytoplasm which contained

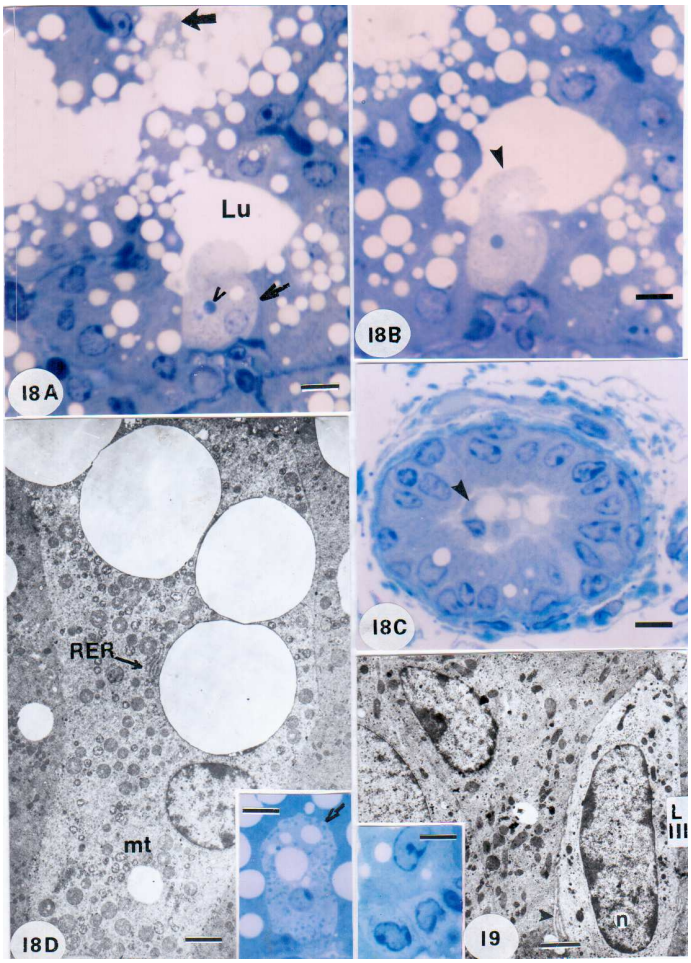

Fig. 18. (A) Semi-thin section in three-week HG showing apical protrusions extending from a type II light cell (arrow) which contains a large dark secretory granule (arrow). Toluidin blue, x 400. Bar, 5 µm. **(B)** Semi-thin section subsequent to the previous image showing the apical protrusion extending into the lumen (arrowhead). Toluidin blue, x 400. Bar, 25 µm. **(C)** Semi-thin section in three-week HG showing an interlobular duct containing luminal remnants of cells with nuclei (arrowhead). Toluidin blue, x 400. Bar, 25 µm. **(D)** TEM from two-week HG showing a type II light cell with large lipid vacuoles. x 3,500. Bar, 2.8 µm. Inset: Semi-thin section in three week HG showing type III light cells (LIII). Toluidine blue, x 1000. Bar, 10 µm.

Fig. 19. TEM from two-week HG showing a type III light cell (LIII) containing an oval nucleus (n) with a few peripheral heterochromatin clumps and a scanty electron lucent cytoplasm containing a few organelles. x 5,200. Bar, 1.8 µm. Inset: Semi-thin section in two week HG showing type III light cells. Toluidine blue, x 1000. Bar, 10 µm.

relatively small nuclei and occasional large and dark granules (Figs. 18 A, B). Their apical cytoplasm protruded into the lumina (Figs. 18 A, B), whereas others may appear rupturing into the lumina (Fig. 18A). The lumina of intraparenchymal ducts may reveal cell remnants containing nuclei (Fig. 18C). In ultrastructure, the cytoplasm of type II light cells exhibited a moderate RER, a marked increase in vesicular SER, mitochondria which may possess electron lucent matrix and lipid vacuoles (Fig. 18D). Type III light cells became larger in size and lighter in staining than the previous age (Fig. 19 inset). Ultrastructure revealed euchromatic nuclei with regular outline surrounded by electron-lucent cytoplasm containing less free ribosomes than the previous age (Fig. 19).

Dark cells revealed more developed cytoplasmic organelles, as well as developed stacks of RER, moderate Golgi bodies, reduction in free ribosomes, an increase in electron dense secretory granules, SER, coated vesicles and electron dense mitochondria. The nuclei were euchromatic with prominent nucleoli (Figs. 20, 21).

Myoepithelial cells with light cytoplasm and those showing mitotic figure became less frequent than in the previous age. The dark type exhibited

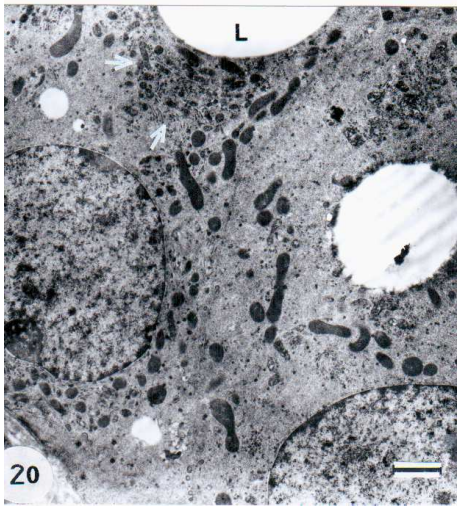

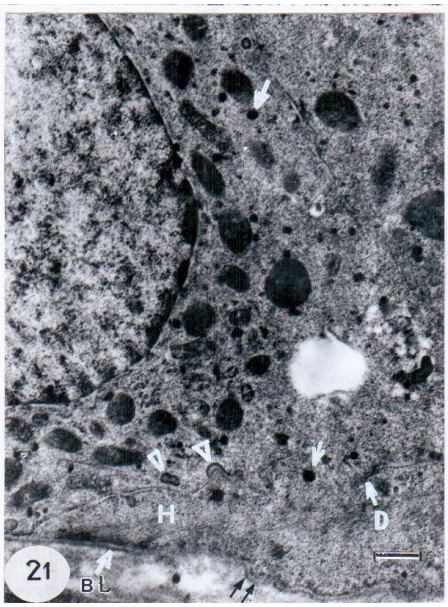

Fig. 20. TEM from two-week HG for a dark cell showing cytoplasmic groups of free ribosome, RER and mitochondria (arrow) and lipid droplets (L). x 4,000. Bar, 2.5 µm.

Fig. 21. Higher magnification for the basal part of the previous figure showing cytoplasmic electron-dense granules (arrows), coated vesicle (arrowheads), desmosome (D) between the basal surface of the dark cell and a myoepithelial cell process which also shows a hemidesmosome (H) attaching it to the basal lamina (BL) and a corrugated basal surface (double arrows). x 10,000. Bar, 1 µm.

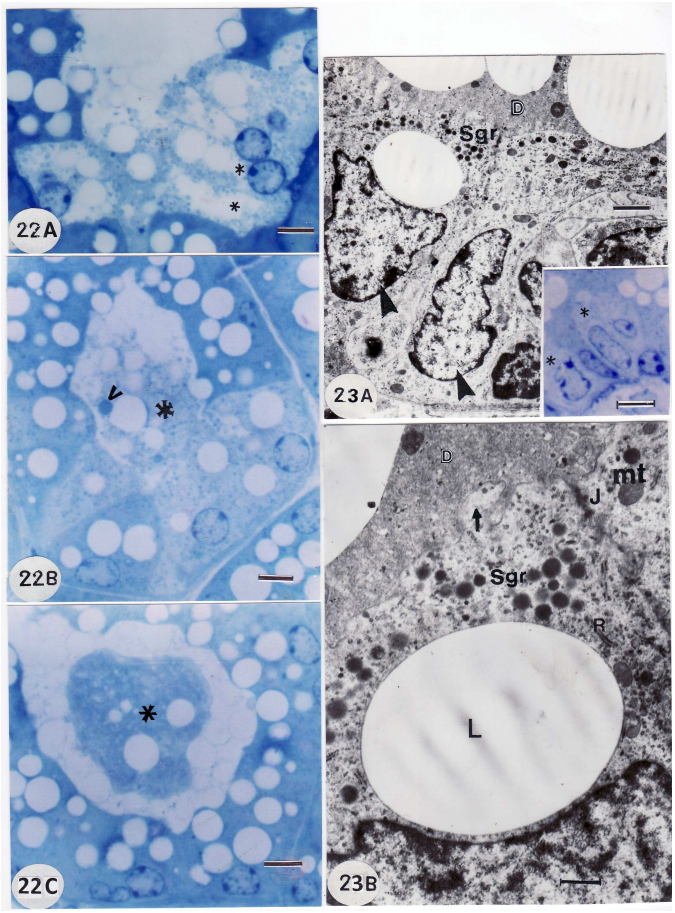

Fig. 22. (A) Semi-thin section in two-month HG showing type II light cells with granular cytoplasm containing fusing cytoplasmic lipid vacuoles (asterisk). Toluidine blue, x 1000. Bar, 10 µm. **(B)** Semi-thin section in two-month HG showing parts of type II light cells within the lumen (asterisk) containing a large dark cytoplasmic granule (arrowhead). Toluidine blue, x 1000. Bar, 10 µm. **(C)** Semi-thin section in two-month HG showing luminal degenerating cellular remnants (asterisk). Toluidine blue, x 1000. Bar, 10 µm.

Fig. 23. (A) TEM from two-month HG showing type III light cells (arrowhead) with apical cytoplasmic secretory granules (Sgr) and a dark cell (D). x 3,500. Bar, 2.8 µm. Inset: semi-thin section in two month HG showing type III light cells (asterisks). Toluidine blue, x 1000. Bar, 10 µm. **(B)** Magnified part of the previous figure showing surface processes (arrows) projecting to an overlying dark cell (D), junctional complex (J), secretory granules (Sgr), mitochondria (mt), short segments of RER (R) and lipid vacuole (L). x 10,400. Bar, 0.9 µm.

Fig. 24. TEM from two-month HG showing a dark cell containing numerous mitochondria (mt) of variable electron density. x 2,700. Bar, 3.7 µm. Inset: higher magnification for condensed (arrowhead) mitochondria (mt). x 14,000. Bar, 0.7 µm.

Fig. 25. (A) Paraffin section in two-month HG showing luminal PAS positive vacuolated secretory material. x 1000. Bar, 10 µm. **(B)** TEM from two-month HG showing luminal membrane-bound apocrine secretory products. x 2,900. Bar, 3.7 µm. © TEM from two month HG showing luminal non membrane-bound electron-lucent cytoplasmic fragments. x 2,900. Bar, 3.7 µm.

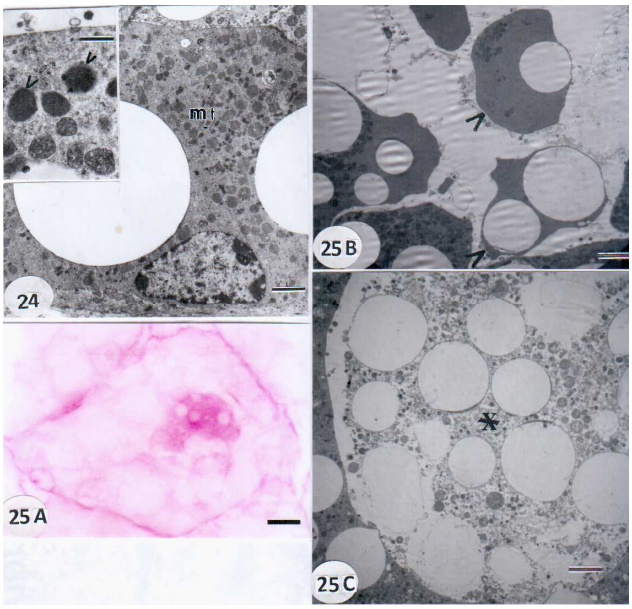

reduction in free ribosomes, an increase in densely packed filaments which formed the main cytoplasmic organelle at both ends of the nucleus and in a thin shell around it. Other organelles included mitochondria, short RER strands and dense bodies. Microfolds extended from their apical plasma membrane into complementary invaginations of the secretory cells, and their basal surface might reveal corrugated surface (Fig. 21) Desmosomes attached myoepithelial cells together and to the overlying epithelial cells. Hemidesmosomes connected them to the underlying basement (Fig. 21).

Lymphocytes were frequently encountered within the secretory end pieces.

Months one to two

Type I light cells were occasionally observed. ***Type II light cells*** became enlarged and exhibited voluminous cytoplasm which may reveal fusion of the lipid vacuoles (Fig. 22A). Their cytoplasm was studded with fine pale granules and a few, large dark granules (Figs. 22A, B). Large parts of the cytoplasm were frequently detected in the lumina of the secretory end pieces (Fig. 22B), where they consequently undergo darkening and degeneration (Fig. 22C). In ultrastructure the nuclei revealed dilated perinuclear cisternae and the cytoplasm contained dilated RER, numerous vesicular SER and numerous mitochondria which usually exhibit electron lucent matrix. ***Type III light cells*** became larger and paler compared with the previous age with light, basal and ovoid nuclei (Fig. 23A inset). Ultrastructurally, the nuclei exhibited less heterochromatin and the surrounding cytoplasm became more electron-lucent than that of the previous age. They were observed to be well equipped with cytoplasmic organelles, mainly mitochondria, lysosomal

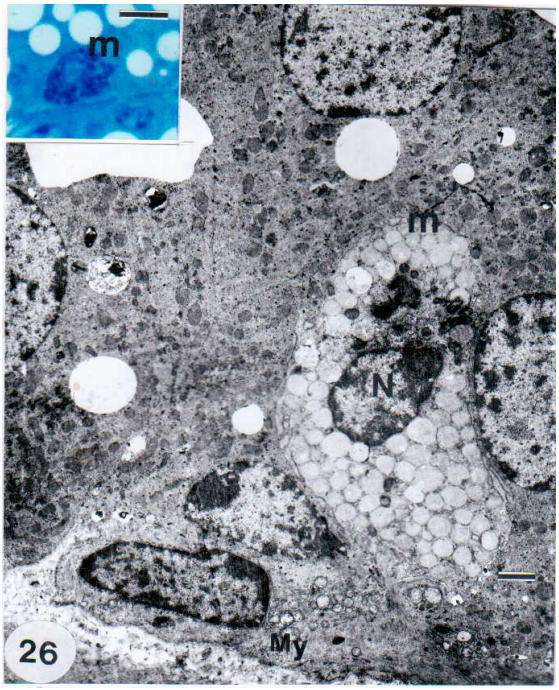

Fig. 26. TEM from two-month HG showing an intraepithelial mast cell (m) containing numerous cytoplasmic secretory granules of low electron density. x 2,700. Bar, 3 µm. Inset: semi-thin section showing an intraepithelial mast cell (m) with numerous metachromatic secretory granules. Toluidine blue, x 1000. Bar, 10 µm.

bodies, RER and Golgi bodies. In addition, a few typical supra-nuclear neuroendocrine secretion granules appeared (Figs. 23 A, B). They were displaying a fine structure that was rather commonplace, an electron dense, homogeneous core of non-crystalline shape, surrounded by a thin granule membrane.

Dark cells cytoplasm contained well developed RER, numerous vesicular SER and numerous mitochondria with electron dense matrix. The latter possessed preserved normal structure with intact cristae (Fig. 24).The secretory material in the lumina of the secretory end pieces may reveal PAS positive (Fig. 25A), AB negative and green colour in Masson's trichrome. In ultrastructure, the membrane-bound apical protrusions are pinched off into the lumina (Fig. 25B) and the somata of cells possessing morphological features similar to type II light cells (electron lucent vacuolated cytoplasm containing numerous mitochondria with damaged cristae) and containing lysosomal-like dense bodies were detected in the lumina (Fig. 25C).

Myoepithelial cells of the light type and their mitotic figures were rare. The dark type revealed more processes, cytoplasmic bundles of packed filaments and coated vesicles along both the basal and apical plasma membranes.

By the age of two month, the secretory end pieces frequently revealed presence of mast cells among their lining epithelium. These mast cells exhibited numerous cytoplasmic metachromatic secretory granules (Fig. 26, inset). In ultrastructure

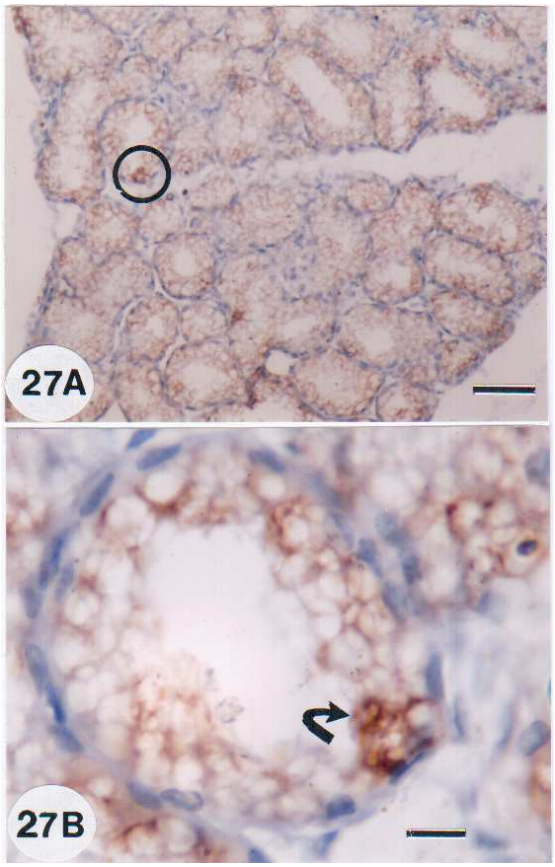

Fig. 27. (A) Paraffin section in two-month HG showing immunoreactivity for chromogranin A in some cells (O). x 40. Bar, 25 µm. **(B)** Higher magnification of the previous image showing a cell which is chromogranin A immunoreactive (arrowhead). x 400. Bar, 2.5 µm.

the secretory granules were of low electron-density (Fig. 26).

Lymphocytes were also encountered within the secretory end pieces.

Immunohistochemistry

Use of chromogranin A antibodies revealed a negative reaction at birth, whereas a week positive reaction was observed at one and two week. With development, a strong positive reaction was observed by the age of one-two month (Figs. 27A, B).

DISCUSSION

This work demonstrated that the female guinea pig HG is secretory at birth. However, it was immature in structure and its secretory cells undergo maturation during the first three weeks postnatal. The gland and its secretory cells continue their growth up to the age of two months postnatal. The main secretory material of the mammalian HG is lipids (Paule, 1957; Sakai, 1981) and the biochemistry of the guinea pig Harderian lipids have been extensively studied (Yamazaki et al., 1981; Seyama et al., 1983, 1984). Although Gasser et al. (2011) recorded negative staining with PAS in

guinea pig HG, we demonstrated in this work that the secretory material of guinea pig HG may include some neutral mucin as confirmed by the positive PAS, negative AB reaction, metachromatic stained material and the green colour detected by Masson's trichrome stain in the lumina and or cytoplasmic vacuoles of some secretory end pieces. Green staining with Masson's trichrome stain is an indicative of the presence of mucin that is a heavily glycosylated protein (Drury and Wallington, 1980). Gasser et al. (2011) did not record neither the age nor the sex of the guinea pig used in their study. The PAS positive secretory material found in our work could be correlated with the electron-dense granular secretory material detected in ultrastructure. The presence of granular dense material similar to that found in this study has been described in the HG of South American armadillo (Aldana and Affani, 2005).

In previous studies by other investigators, two or three types of glandular cells have been morphologically distinguished in various rodents: the mouse (Strum and Shear, 1982; Watanabe, 1980; Woodhouse and Rhodin, 1963), the rat (Brownsheidle and Niewenhuis, 1978; Carrier, 1985; Tsutsumi et al., 1966) the plain mouse (Johnston et al., 1985) and the male golden hamster (Bucana and Nadakavukaren, 1973; Hoffman, 1971; Lopez et al., 1993). However, in the guinea pig we distinguished four types of cells with different characteristic morphological features. Detection of dark and light cells have been reported frequently in many tissues as developing hamster HG (Lopez et al., 1992), adult rat vomeronasal organ (Eltony and Elgayar, 2011) and developing rabbit VNO (Elgayar et al., 2014). Presence of more than one cell type in many HGs has often been interpreted as being one cell type in different activity levels (Payne et al., 1994; Lopez et al., 1996). This hypothesis could be applicable for light and dark myoepithelial cells detected in the guinea pig. This is in agreement with the work of Nagashima and Ono (1985) who considered the light myoepithelial cells in human submandibular gland as an immature type. However, type I light cells could represent undifferentiated cells capable of undergoing division. In support of this view, their gradual decrease in frequency coincides with the gradual decrease in mitotic figures observed among the secretory cells. In addition, they possess large size and large light nuclei and there is evidence that the cell volume of growing cells is proportional to the amount of DNA in the nucleus (Horner and Macgregor, 1983) and the diploid cells are twice the size of haploid cells (Swanson et al., 1991).

The morphological features of myoepithelial cells in this work are in accordance with the study of Satoh et al. (1994). These authors suggested that their function is to maintain the contour of the glandular endpieces, serving as the exoskeleton of the endpieces. However, the cytological features are consistent with the function of the myoepithelial cell mainly as a contractile element, and possibly as a regulator for fluid transport. They are attached to the glandular cells of the end-pieces with desmosomes and interdigitating cytoplasmic processes. Densely packed myofilaments fill most of the cytoplasm, and coated vesicles on the inner and outer borders are prevalent.

Chromogranin has been found to be a ubiquitous protein stored in dense-core secretory granules of the endocrine, exocrine, and nervous systems. This observation was confirmed by detection of CgA positive reacting cells by immunohistochemistry among the gland secretory epithelial cells. CgA present in endocrine cells serve as a marker for large secretory granules with electron dense cores (Taupenot et al., 2002). It belongs to the granin family of acidic secretory glycoproteins that are expressed in most types of normal neuroendocrine cells (c.f. Nobels et al., 1998; Wick, 2000). Cg A is typically bound to the membrane of the neuroendocrine secretion granules. Many of the listed chromogranin fragments act by means of autocrine and paracrine in endocrine, cardiovascular and nervous system (Jiang et al., 2001). According to Taupenot et al. (2002), cells present in non-endocrine organs produce highly active chemical substances (biogenic and peptide amines) responsible for local regulation.

According to the objective ultrastructure criteria, the electron-dense secretory granules present in type III light cells may be sources of CgA which we detected by immunohistochemistry in cells disseminated among the epithelium lining the glandular secretory end pieces. The age by which type III light cells reached complete maturation coincided with the time of sexual maturation may lead one to suggest presence of mutual relation. However, CgA is also found to be expressed and released from exocrine serous acinar cells of the human submandibular salivary glands of human (Saruta et al., 2005), and its processed products have been shown to have a role in immunity against microbes (Metz-Boutigue, 2003). Therefore, immunoelectron microscopic technique is necessary to verify that type III cell is the CgA producing cell.

The newborn dark cells were morphologically at an advanced stage of development, as evidenced by the secretory activity of the newborn gland. During early stages of maturation, the dark cells revealed nucleolus-like bodies which were similar to those described in various cell types including oocytes (Azavedo, 1984), spermatocytes (Fuge, 1976), embryonic cells (Takeuchi, 1980), pinealocytes (Fechner, 1986) as well as in developing hamster HG (Lopez et al., 1990). This finding may lead one to suggest their being a transient store of ribonucleoprotein during periods of rapid metabolism and differentiation as in embryonic ectodermal cells (Takeuchi and Takeuchi, 1982).

The difference in the configuration of the secreto-

ry granules in dark cells indicates difference in their products. The gradual increase in frequency of condensed mitochondria in dark cells, with development, could be related to the energy and metabolic requirements during development. The density of mitochondria generally depends on cellular requirement of ATP and differs significantly from one cell type to another (Veltri et al., 1990). In accordance with our findings, Baccari et al. (2004) reported that the condensed configuration observed in the hyperthyroid rat HG indicated increased phosphorylative activity. It is noteworthy to mention that in guinea pig HG mitochondria, in addition to synthesizing ATP required for the maintenance of aerobic life, share peroxisomes the process of oxidation of fatty acids and it is proved that mitochondria possess distinct fatty acyl Co-A synthetase enzyme (Kono et al., 1996).

In female guinea pig HG, all modes of secretion (merocrine, apocrine and holocrine) have been observed in this work. The detection of the lipid vacuoles fusing with the apical plasma membrane and the discharge of their contents into the lumen were indicative of merocrine mode of secretion. These findings are in agreement with the hypothesis proposed by several authors concerning the merocrine nature of HG secretion (Watanabe, 1980; Sakai and Yohro, 1981; Lopez et al., 1992a). However, neither the apocrine or holocrine modes of secretion have been previously reported in guinea pig HG. Satoh et al. (1996) elicited the presence of merocrine cell discharge in male guinea pig HG by high doses of carbacol. The apocrine mode of secretion was evident in this study by detection of apical protrusions and/or membrane bounded cytoplasmic fragments in the lumen which were extending from the dark and/or type II light cells. The physiological significance of the occurrence of both exocytosis and apocrine secretory mechanisms in a single cell is not clearly known. Cristofoletti et al. (2001) reported that it may indicate that the glandular cells synthesize both apocrine secreted substances and those released via exocytosis. Holocrine release was evident in female guinea pig by detection of rupturing type II light cells and the detection of their cytoplasmic fragments, which were non-membrane bound, in the lumina. These cells characteristically possessed morphological features characteristic of dying cells specifically voluminous cytoplasm, large lipid vacuoles and huge amount of mitochondria with electron lucent matrix. In the rat, Carrier (1985) reported that cells with large lipid vacuoles were in fact dying cells, and that this formed a holocrine mechanism by which gland products were released. Similar findings have been reported in HG of golden hamsters (Hoffman, 1971) and wistar rat (Djeridane, 1994). However, the holocrine mode of secretion was not the main contributor of secretion. In conclusion, the female guinea pig HG is an actively secreting gland since birth, completes its development by the age of two month and possesses many characteristic morphological features.

ACKNOWLEDGEMENTS

No conflicts of interests have been declared. Assiut University is the source of funding for this research.

REFERENCES

ALDANA MHJ, AFFANNI JM (2005) Anatomy, histology, histochemistry and fine structure of the Harderian gland in the South American armadillo *Chaetophractus villosus* (Xenarthra,Mammalia). *Anat Embryol*, 209(5): 409-424.

AZAVEDO C (1984) Developmental and ultrastructural autoradiographic studies of nucleolus-like bodies (nuages) in oocyte of a viviparous teleost (*xiphophorus helleri*). *Cell Tissue Res*, 238: 121-128.

BACCARI GC, MONTEFORTE R, De LANGE P, RAUCCI F, FARINA F, LANNI A (2004) Thyroid hormone affects secretory activity and uncoupling protein-3 expression in rat Harderian gland. *Endocrinology*, 145 (7): 3338-3345.

BROWNSCHEIDLE CM, NIUWENHUIS RJ (1978) Ultrastructure of the Harderian gland in male albino rats. *Anat Rec*, 190: 735-754.

BUCANA CD, NADAKAVUKAREN MJ (1973) Ultrastructural observations of postnatal development of the hamster harderian gland. II. Male and female. *Z. Zellforsch*, 142: 1-12.

CARRIERE R (1985) Ultrastructural visualization of intracellular porphyrin in the rat Harderian gland. *Anat Rec*, 213: 496-504.

CHIEFF G, MENUCCI S, DI MATTEO L (1993) The orbital glands of the terrapin Peseudemys ScriptalIn response to osmotic stress: A light and electron microscopic study. *J Anat*, 183: 21-33.

CHIEFFI G, BACCARI GC, DI MATTEO L, D'ISTRIA M, MINUCCI S, VARRIALE B (1996) Cell biology of the Harderian gland. *Int Rev Cytol*, 168: 1-80.

CHITANO P, WANG J, COX CM, STEPHENS NL, MURPHY TM (2000) Different ontogeny of rate of force generation and shortening velocity in guinea pig trachealis. *J Appl Physiol*, 88: 1338-1345.

CRISTOFOLETTI PT, RIBEIRO AF, TERRA WR (2001) Apocrine secretion of amylase and exocytosis of trypsin along the midgut of Tenebrio molitor larvae. *J Insect Physiol*, 47: 143-155.

DJERIDANE Y (1994) The harderian gland and its excretory duct in the Wistar rat. A histological and ultrastructural study. *J Anat*, 184: 553-566.

DRURY RAB, WALLINGTON EA (1980) Carelton's Histology Technique, 5th edition. Oxford University Press, Oxford. New York, Toronto.

ELGAYAR SA, ELTONY SA, OTHMAN MA (2014) Morphology of non-sensory epithelium during post-natal development of the rabbit vomeronasal organ. doi: 10.1111/ahe.12073

ELTONY SA, ELGAYAR SA (2011) Morphology of the non-sensory tissue components in rat aging vomeronasal organ. *Anat Histol Embryol*, 40: 263-277.

GASSER K, FUCHS-BAUMGARTINGER A, TICH Y, NELL B (2011) Investigations on the conjunctival goblet cells and on the characteristics of glands associated with the eye in the guinea pig. *Vet Ophthalmol*, 14 (1): 26-40.

GUPTA PD (1983) Ultrastructure study on semithin section. *Science Tools*, 30: 6-7.

HOFFMAN RA (1971) Influence of some endocrine glands, hormones, and blinding on the histology and porphyrins of the Harderian glands of golden hamsters. *Am J Anat*, 132: 463-478.

HORNER HA, MACGREGOR HC (1983) C Value and cell volume: their significance in the evolution and development of amphibians. *J Cell Sci*, 63: 135-146.

JIANG Q, TAUPENOT L, MAHATA M, MAHATA SK, O'CONNER DT, MILES LA, PARMER RJ (2001) Proteolytic cleavage of chromogranin A (CgA) by plasmin. Selective liberation of a bioactive CgA fragment that regulates catecholamine release. *J Biol Chem*, 276: 25022-25029.

KONO M, HORI C, HASHIMOTO T, HORI S, SEYAMA Y (1996) Two distinct long-chain-acyl-CoA synthetases in guinea pig harderian gland. *Eur J Biochem*, 238: 104-111.

LOPEZ JM, TOLIVIA CD, ALVAREZ-LORIA M (1990) Ultrastructural study of lamellar and nucleolus-like bodies in the Harderian gland during postnatal development of the Hamster (Mesocricetusauratus). *Anat Rec*, 228: 247-254.

LOPEZ JM, TOLIVIA J, ALVAREZ-URIA M (1992a) Postnatal development of the Harderian gland in the Syrian golden Hamster (Mesocricetus auratus): A light and electron microscopic study. *Anat Rec*, 233: 597-616.

LOPEZ JM, TOLIVIA J, ALVAREZ-URIA M (1992b) An ultrastructural study myoepithelium maturation during postnatal development of the hamster Harderian gland. *Anat Embryol*, 186: 573-582.

LOPEZ JM, TOLIVIA J, ALVAREZ-URIA M, PAYNE AP, MCGADEY J, MOORE MR (1993) An electron microscopic study of the Harderian gland of the Syrian Hamster with particular references to the process of formation and discharge of the secretory vacuoles. *Anat Rec*, 233(3): 342-352.

LOPEZ JM, CARBAJO-PEREZ E, FERNANDEZ-SUAREZ A, ALVAREZ-URIA M (1996) Postnatal development of cell types in the hamster Harderian gland. *Micr Res Tech*, 34: 48-54.

MENENDEZ-PELAEZ A, MAYO JC, SAINZ RM, PEREZ M, ANTOLIN I, TOLIVIA D (1992) Development and hormonal regulation of mast cells in the Harderian gland of Syrian hamsters. *Anat Embryol*, 186 (1): 91-97.

METZ-BOUTIGUE MH, KIEFFER AE, GOUMON Y, AUNIS D (2003) Innate immunity: involvement of new neuropeptides [review]. *Trends Microbiol*, 11: 585-592.

MULLER HB (1969) The postnatal development of the rat harderian gland. II. Enzyme-histochemical studies. *Histochemie*, 20(2): 181-196.

NAGASHIMA Y, ONO K (1985) Myoepithelial cell ultrastructure in the submandibular gland of man. *Anat Embryol*, 171: 259-265.

NOBELS FRE, KWEKKEBOOM DJ, BOUILLON R, LAMBERTS SWJ (1998) Chromogranin A: its clinical value as marker of neuroendocrine tumours. *Eur J Clin Invest*, 28: 431-440.

PADILLA-CARLIN DJ, MC MURRAY DN, HICKEY AJ (2008) The guinea pig as a model of infectious diseases. *Comp Med*, 58(4): 324-340.

PAULE WJ (1957) The comparative histochemistry of the Harderian Gland. Ph. D. Dissertation. Publisher, Ohio State University.

PAYNE AP (1994) The Harderian gland. A tercentineal review. *J Anat*, 185: 1-49.

REYNOLDS ES (1963) The use of lead citrate at high pH as an electron opaque stain in electron microscopy. *J Cell Biol*, 17: 208-212.

SAKAI T (1992) Comparative anatomy of the mammalian Harderian glands. In: Webb SM, Hoffman RA, Puig-Domingo ML, Reiter RJ (Eds): *Harderian glands: porphyrin, metabolism, behavioral and endocrine effects*. Springer, Berlin, pp 7-23.

SAKAI T, YOHRO T (1981) A histological study of the Harderian gland of mongolian gerbils, *meriones meridians*. *Anat Rec*, 200: 259-270.

SARUTA J, TSUKINOKI K, SASAQURI K, ISHII H, YASUDA M, OSAMURA YR, SATO S (2005) Expression and localization of chromogranin A gene and protein in human submandibular gland. *Cells Tissues Organs*, 180(4): 237-244.

SATOH Y, HABARA Y, KANNO Y, ONO K (1993) Carbamyl cholin-induced morphological changes and spatial dynamics of Ca in Harderian gland of guinea pigs. Calcium-dependent lipid secretion and contraction of myoepithelial cells. *Cell Tissue Res*, 274: 1-14.

SEYAMA Y, OTSUKA H, KAWAGUCHI A, YAMAKAWA T (1981) Fatty acid synthetase from the harderian gland of guinea pig, biosynthesis of methyl- branched fatty acids. *J Biochem*, 90: 789-797.

SEYAMA Y, OHASHI K, YASUGI E, OTSUKA H (1984) Fatty acid composition from guinea pig Harderian gland. *J Biochem*, 96: 1639-1643.

SEYAMA Y, OTSUKA H, OHASHI K, VIVIEN-ROELS B, PEVET P (1995) Sexual dimorphism of lipids in Harderian glands of golden hamsters. *J Biochem*, 117(3): 661-670.

SMELSER GK (1943) Changes included in the Harderian gland of the guinea pig by the injection of hypophyseal extracts. *Anat Rec*, 86: 41-57.

STRUM JM, SHEAR CR (1982) Harderian glands in mice: fluorescence, peroxidase activity and fine structure. *Tissue Cell*, 14: 135-148.

SWANSON JA, MELINDA L, PHILIP EK (1991) Cellular dimensions affecting the nucleocytoplasmic volume ratio. *J Cell Biol*, 115: 941-948.

TAKEUCHI IK (1980) Nucleolus-like bodies in the em-

bryonic ectodermal and mesodermal cells of post implantation rat embryos. *J Electron Microsc*, 29: 186-189.

TAKEUCHI IK, TAKEUCHI YK (1982) Ultrastructural and cytochemical studies on nucleolus-like bodies in early post implantation rat embryos. *Cell Tissue Res*, 226: 257-266.

TAUPENOT L, HARPER KL, MAHAPATRA NR, PARMER RJ, MAHATA SK, O'CONNER DT (2002) Identification of a novel sorting determinant for the regulated pathway in the secretory protein chromogranin A. *J Cell Science*, 115: 4827-4841.

TSUTSUMI A, IWATA K, OGAWA K, MASTSUURA K (1966) Histochemical and electron microscopic observations on the Harderian gland of albino rat. *Arch Histol Jpn*, 27: 553-567.

VELTRI KL, ESPIRITU M, SINGH G (1990) Distinct genomic copy number in mitochondria of different mammalian organs. *J Cell Physiol*, 143: 160-164.

WATANABE M (1980) An autoradiographic biochemical and morphological study of the Harderian gland of mouse. *J Morphol*, 163: 349-365.

WICK MR (2000) Immunohistology of neuroendocrine and neuro ectodermal tumors. *Semin Diagn Pathol*, 17: 194-203.

WETTERBERG L, YUWILER A, GELLER E, SCHAPIRO S (1970) Harderian gland: Development and influence of early hormonal treatment on porphyrin content. *Science*, 168 (3934): 996-998.

YAMAZAKI T, SEYAMA Y, OTSUKA H, YAMAKAWA T (1981) Identification of alkyldiacylglycerols containing saturated methyl branched chains in the Harderian gland of guinea pig. *J Biochem*, 89: 683-691.